Published in final edited form as:

Mol Pharm. 2015 October 05; 12(10): 3527–3534. doi:10.1021/acs.molpharmaceut.5b00105.

PET Imaging of Dll4 Expression in Glioblastoma and Colorectal Cancer Xenografts Using ^{64}Cu-Labeled Monoclonal Antibody 61B

Bin Zhou[†,‡], **Hui Wang**[‡], **Ren Liu**[§], **Mengzhe Wang**[‡], **Huaifu Deng**[‡], **Benjamin C. Giglio**[‡], **Parkash S. Gill**[§], **Hong Shan**[*,†,‖], and **Zibo Li**[*,‡]

[†]Department of Radiology, The Third Affiliated Hospital of Sun Yat-sen University, Guangzhou 510630, China

[‡]Biomedical Research Imaging Center, Department of Radiology, University of North Carolina, Chapel Hill, North Carolina 27514, United States

[§]Department of Pathology, University of Southern California, Los Angeles, California 90033, United States

[‖]Interventional Radiology Institute, Sun Yat-sen University, Guangzhou 510630, China

Abstract

Delta-like ligand 4 (Dll4) expressed in tumor cells plays a key role to promote tumor growth of numerous cancer types. Based on a novel antihuman Dll4 monoclonal antibody (61B), we developed a ^{64}Cu-labeled probe for positron emission tomography (PET) imaging of tumor Dll4 expression. In this study, 61B was conjugated with the ^{64}Cu-chelator DOTA through lysine on the antibody. Human IgG (hIgG)-DOTA, which did not bind to Dll4, was also prepared as a control. The Dll4 binding activity of the probes was evaluated through the bead-based binding assay with Dll4-alkaline phosphatase. The resulting PET probes were evaluated in U87MG glioblastoma and HT29 colorectal cancer xenografts in athymic nude mice. Our results demonstrated that the 61B-DOTA retained (77.2 ± 3.7) % Dll4 binding activity of the unmodified 61B, which is significantly higher than that of hIgG-DOTA (0.06 ± 0.03) %. Confocal microscopy analysis confirmed that 61B-Cy5.5, but not IgG-Cy5.5, predominantly located within the U87MG and HT29 cells cytoplasm. U87MG cells showed higher 61B-Cy5.5 binding as compared to HT29 cells. In U87MG xenografts, 61B-DOTA-^{64}Cu demonstrated remarkable tumor accumulation (10.5 ± 1.7 and 10.2 ± 1.2%ID/g at 24 and 48 h postinjection, respectively). In HT29 xenografts, tumor accumulation of 61B-DOTA-^{64}Cu was significantly lower than that of U87MG (7.3 ± 1.3 and 6.6 ± 1.3%ID/g at 24 and 48 h postinjection, respectively). The tumor accumulation of 61B-DOTA-^{64}Cu was significantly higher than that of hIgG-DOTA-^{64}Cu in both xenografts models. Immunofluorescence staining of the tumor tissues further confirmed that tumor accumulation of 61B-Cy5.5 was correlated well with in vivo PET imaging data using 61B-DOTA-^{64}Cu. In

[*]Corresponding Authors: Address: Department of Radiology, The Third Affiliated Hospital of Sun Yat-sen University, 600 Tianhe Road, Guangzhou, 510630, China. Tel: +86 20-85252573. Fax: +86 20-85252573. shanhong@mail.sysu.edu.cn. [*]Address: Department of Radiology and Biomedical Research Imaging Center, University of North Carolina-Chapel Hill, 125 Mason Farm Road, Chapel Hill, North Carolina 27599, United States. Tel: +1(919) 962-5152. Fax: +1(919) 843-4456. zibo_li@med.unc.edu.

Supporting Information: The Supporting Information is available free of charge on the ACS Publications website at DOI: 10.1021/acs.molpharmaceut.5b00105.

Notes: The authors declare no competing financial interest.

conclusion, 61B-DOTA-^{64}Cu PET probe was successfully synthesized and demonstrated prominent tumor uptake by targeting Dll4. 61B-DOTA-^{64}Cu has great potential to be used for noninvasive Dll4 imaging, which could be valuable for tumor detection, Dll4 expression level evaluation, and Dll4-based treatment monitoring.

Graphical abstract

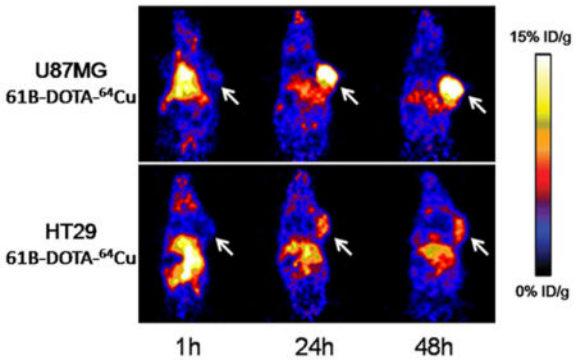

Keywords

Dll4; glioblastoma; colorectal cancer; ^{64}Cu; microPET

Introduction

The Notch family of proteins is composed of four transmembrane receptors (Notch 1, 2, 3, and 4), which are activated by five known membrane-anchored ligands (jagged 1 and 2 and delta-like ligand Dll1, 3, and 4).[1] Among these, Dll4 has recently appeared as a critical regulator of tumor angiogenesis. When expressed in tumor cells, Dll4 was found to activate Notch signaling, increase blood vessel size, and improve tumor vascular function in various cancer types.[2]

Based on its important role in cancer progression, Dll4 targeted therapy became a promising treatment strategy for patient management. Emerging evidence suggested that the blockage of Dll4 led to broad spectrum antitumor activity in cancer cell line-based xenograft models.[3–5] For example, soluble forms of Dll4 interrupted Dll4-Notch signaling pathway and led to decreased tumor growth.[3] More importantly, Dll4 overexpression was suggested to be an independent predictor of poor survival in malignant tumor.[3] Combination therapy with Dll4 antibody and ionizing radiation or ultrasound-stimulated microbubbles resulted in extensive tumor necrosis and enhanced tumor growth delay in mice xenografts.[6,7] Combining Dll4-targeted siRNA with bevacizumab also resulted in greater inhibition of tumor growth.[8] Despite the encouraging results, not all the patients will benefit from Dll4-tagreted therapy due to heterogeneous Dll4 expression levels; in addition, the Dll4 expression level may change during such targeted therapy, which may affect therapeutic efficacy and require the adjustment of treatment regime. Therefore, quantitative analysis of Dll4 expression in living subjects may greatly facilitate patient selection and treatment

response monitoring. Despite the critical need, research on robust, quantitative, and noninvasive imaging methods to visualize Dll4 expression in vivo are still very limited.[9]

Positron emission tomography (PET) is a highly sensitive, noninvasive, and quantitative technique that has been used widely for imaging biomarker distribution, concentration, and functions in vivo under normal and pathological conditions. In this study, we aimed to develop a ^{64}Cu labeled humanized monoclonal Dll4 antibody (61B) for human Dll4 imaging. We used two cancer xenograft models to investigate Dll4 expression using PET imaging with the newly developed probe. The resulting PET probe may provide important information on determining the utility of Dll4-targeted chemo- and radiotherapy by selecting the Dll4 positive patients.

Experimental Section

Materials

The antibody 61B and Dll4-alkaline phosphatase (Dll4-AP) were kindly provided by Vasgene Therapeutics Inc. (Los Angeles, CA, USA). 1,4,7,10-Tetra-azacyclododecane-*N*,*N*′,*N*″,*N*‴-tetraacetic acid (DOTA) was purchased from Macrocyclics Inc. (Dallas, TX, USA). PD-10 disposable columns were purchased from GE Healthcare Life Sciences (Piscataway, NJ, USA). Ultra Protein A Resin for binding activity assay was purchased from GenScript USA Inc. (Piscataway, NJ, USA). Human IgG (hIgG) was purchased from Rockland (Gilbertsville, PA, USA).

For immunofluorescence staining, rat antimouse CD31 antibody was purchased from Abcam (Cambridge, MA, USA). Secondary antibody Alexa Fluor 568 Goat Anti-Rat IgG was purchased from Life Technologies (Grand Island, NY, USA). Cy5.5 *N*-hydroxysuccinimide (Cy5.5-NHS) ester was purchased from Lumiprobe Corporation (Hallandale Beach, Florida, USA). ^{64}Cu was produced using the ^{64}Ni(p,n)^{64}Cu nuclear reaction in Washington University and the University of Wisconsin and supplied in high specific activity as $^{64}CuCl_2$ in 0.1 N HCl.

Chemistry and Radiochemistry

61B and hIgG were conjugated with DOTA using a method published previously.[10] Briefly, DOTA was first activated to DOTA-*N*-hydroxysulfo-succinimidyl as reported previously.[10,11] After cooled to 4 °C, the reaction mixture was added to 61B or hIgG in 0.1 M borate buffer (pH 8.5) and incubated at 4 °C overnight. The 61B-DOTA or hIgG-DOTA was purified using a PD-10 column and concentrated by a Centricon filter (Millipore). The concentrations of 61B-DOTA or hIgG-DOTA were measured based on absorbance at 280 nm using unconjugated antibody of known concentrations as a standard. The synthesis of 61B-DOTA-^{64}Cu and hIgG-DOTA-^{64}Cu was performed following procedures described previously.[10] Briefly, 30 μg of the 61B-DOTA-^{64}Cu or hIgG-DOTA-^{64}Cu was loaded to $^{64}CuCl_2$ (37MBq ^{64}Cu per 30 μg antibody). The pH of the reaction mixture was adjusted to 5.5 with 0.1 N acetate buffer and incubated at 40 °C for 1 h with constant shaking. The 61B-DOTA-^{64}Cu or hIgG-DOTA-^{64}Cu was purified by a PD-10 column. The radioactive fraction containing 61B-DOTA-^{64}Cu or hIgG-DOTA-^{64}Cu product was collected for further

experiments. Twenty micro curie of ^{64}Cu-labeled product was loaded onto Centricon with a molecular weight cutoff of 10 000. After initial centrifugation, 0.5 mL of PBS buffer was added followed by additional centrifugation. After final wash, the fraction on top of the centricon (with MW > 10 000 containing 61B-DOTA-^{64}Cu) was collected, and the radioactivity in this fraction was measured using γ-counter. The purity of 61B-DOTA-^{64}Cu was calculated by dividing 61B-DOTA-^{64}Cu associated radioactivity (after centrifugation) with 20 uCi (total product). In addition, 10 μg of 61B-DOTA-^{64}Cu was analyzed by 4–12% NuPAGE Bis-Tris gel. Two gels were run in parallel. After electrophoresis, one gel was stained with SimplyBlue SafeStain for protein purity assessment, and the other gel was analyzed by autoradiography for radioactivity measurement. The radiochemical purity of the final product was further confirmed by comparing these two measurements.

Binding Affinity Assay

To test the Dll4 binding activity of antibody conjugates, 300 ng of Dll4-alkaline phosphatase (AP) was preincubated with 0, 10, 20, 40, 80, or 120 ng of unmodified 61B antibody for 15 min. The formed complex was then immobilized on Protein A Resin (10 μL per tube) for 1 h. Unbound proteins were removed by washing twice with PBS, and precipitated AP activity ($OD_{405\ nm}$ value) was detected on microplate reader after adding *para*-nitro-phenylphosphate (PNPP). A standard curve and formula were derived based on $OD_{405\ nm}$ values and 61B concentrations.[12] To determine Dll4 binding affinity of DOTA-conjugated antibodies, 50 ng of hIgG-DOTA or 61B-DOTA immobilized on Protein A Resin (10 μL per tube) was incubated with 300 ng of Dll4-AP for 1 h. Unbound proteins were removed by washing twice with PBS. The amount of DOTA-conjugates of antibody, which can actively bind to Dll4, was then determined after adding PNPP and calculated according to the formula developed above. Binding activities of DOTA-conjugated antibodies were expressed as the percentage of active 61B-DOTA (equivalent to ng of unmodified 61B) to the total amount of 61B-DOTA. Binding activity of hIgG-DOTA was also calculated accordingly. Each sample was repeated as triplicate.

Synthesis of 61B-Cy5.5 and hIgG-Cy5.5

An aqueous solution of 61B or hIgG (350 μg) was mixed with Cy5.5-NHS in 0.1 M borate buffer (pH 8.5). The molar ratio of antibody to Cy5.5-NHS was 1 to 2.4. After incubated overnight at 4 °C, the reaction mixture was passed through a PD-10 column and eluted with PBS solution.[13] 61B-Cy5.5 or hIgG-Cy5.5 was collected; the absorbance at 280 and 673 nm of 61B-Cy5.5 and hIgG-Cy5.5 were measured with Thermo BioMate 3S spectrophotometers (Thermo Fisher Scientific Inc., Waltham, MA, USA). The dye-to-antibody molar ratio was calculated according to manufacturer's instructions.

Cell Culture and Animal Models

Animal procedures were performed according to protocol approved by the University of North Carolina Institutional Animal Care and Use Committee. Human colorectal cancer cell line HT29 and human glioblastoma cell line U87MG were obtained from American Type Culture Collection (Manassas, VA, USA) and were cultured in RPMI-1640 or DMEM (Gibco, Grand Island, NY, USA) supplemented with 10% fetal bovine serum (FBS) (Omega Scientific, Tarzana, CA, USA), respectively. The cells were maintained at 37 °C in a

humidified atmosphere containing 5% CO_2. Tumor models were established in 4- to 6-week old female athymic nude mice (Harlan, Indianapolis, IN, USA). The 2×10^6 tumor cells suspended in 100 μL of cell culture medium without FBS were inoculated subcutaneously at the right shoulder. The mice were used for microPET imaging studies when the tumor reached about 0.8 cm in diameter (3–4 weeks after cancer cells inoculation).

Tumor Cell Confocal Microscopy Analysis

To test the cell binding with 61B, 5×10^4 U87MG or HT29 cells were seeded in each chamber of an eight-chamber slide (Thermo Fisher Scientific Inc., Waltham, MA, USA) and incubated overnight to allow cell adhesion. After the cells were rinsed with PBS buffer twice, 300 μL of complete culture medium containing 60 nM 61B-Cy5.5 or hIgG-Cy5.5 was added. The cells were incubated for 30 min at 37 °C, followed by PBS buffer washing, and fixed in 4% paraformaldehyde (Electron Microscopy Sciences, Hatfield, PA, USA) for 20 min at room temperature. Subsequently, the cells were covered with EverBrite Mounting Medium with 4,6-diamino-2-phenylindole (DAPI, Biotium, CA, USA) and observed under Zeiss LSM 710 laser scanning microscope (Zeiss, Jena, German).

MicroPET Imaging

MicroPET scans were performed as described previously.[11,14] About 3.7–7.4MBq dose of PET probe (61B-DOTA-^{64}Cu) was intravenously injected into each mouse under isoflurane anesthesia (2–4% for induction and 2% for maintenance in 100% O_2). Static scans were acquired at 1, 24, 48, and 72 h after injection. The images were reconstructed by two-dimensional ordered-subsets expectation maximum. For each microPET scan, regions of interest were drawn over the tumor and major organs on decay-corrected whole-body coronal images. The radioactivity accumulation within tumors or organs was obtained from the mean value within the multiple regions of interest and then converted to percentage injected dose per gram (%ID/g).[15] For both HT29 and U87MG tumor models, hIgG-DOTA-^{64}Cu was used as the control to confirm the receptor specificity of ^{64}Cu-labeled 61B. The tumors of each group ($n = 4$) were size-matched. After all PET scans were performed, the animals were sacrificed; the blood, heart, and other major organs were collected and wet-weighed. The radioactivity in the tissue was measured using a gamma-counter (Packard Instruments). The results are presented as the percentage injected dose per gram of tissue (%ID/g). Values are expressed as the means ± SD for a group of three animals.

Immunofluorescence Staining of Tumor Tissue

To investigate the antibody distribution within tumor tissues, 61B-Cy5.5 or hIgG-Cy5.5 (0.2 nmol) was injected into each mice bearing U87MG or HT29 tumor via tail vein. At 48 h after injection, the mice were euthanized, and the tumors were dissected, embedded in Tissue-Tec optimal-cutting-temperature compound (Sakura Finetek, Torrance, CA, USA) and cut into 8 μm sections. Frozen sections were fixed in ice-cold acetone for 5 min, blocked with 10% normal horse serum (Gibco, Grand Island, NY, USA) for 20 min, and then incubated with primary anti-CD31 antibody at room temperature for 30 min. After PBS buffer washing, the sections were incubated with secondary antibody for 30 min at room temperature. Subsequently, the slides were covered with EverBrite Mounting Medium containing DAPI and observed under Zeiss LSM 710 laser scanning microscope.

Statistical Analysis

Quantitative data are expressed as mean ± SD. Means were compared using one-way ANOVA and the Student's *t* test. *p* values less than 0.05 were considered statistically significant.

Results

Chemistry, Radiochemistry, and Binding Activity Assay

61B and hIgG were conjugated with ^{64}Cu chelator DOTA through amino groups. The resultant 61B-DOTA and hIgG-DOTA were labeled with ^{64}Cu as described. The radiochemical yields were 65.6% and 53.4% for 61B-DOTA-^{64}Cu and hIgG-DOTA-^{64}Cu, respectively. Based on centrifugation experiment, 99.8% of radioactivity in final labeling product was associated with 61B-DOTA-^{64}Cu; and the free ^{64}Cu was only 0.2% of the final product. In addition, 10 μg of 61B-DOTA-^{64}Cu gave a single band on NuPAGE gel with approximate molecular weight of 150 kDa; and this signal was well-associated with most of the radioactivity detected by autoradiography (Supplementary Figure 2). These results further confirmed that 61B antibody integrity was retained during DOTA conjugation and ^{64}Cu labeling, and the 61B-DOTA-^{64}Cu has high radiochemical purity after purification. The calculated specific activity of 61B-DOTA-^{64}Cu and hIgG-DOTA-^{64}Cu were 121 and 98 MBq/μmol, respectively. To study the impact of DOTA-conjugation on Dll4 binding ability, a binding affinity assay was performed. Based on $OD_{405\ nm}$ values and 61B concentrations, Formula 1 was derived. Compared with unlabeled 61B, 61B-DOTA retained (77.2 ± 3.7) % of Dll4 binding ability; while hIgG-DOTA only had background level of Dll4 binding ability ((0.06 ± 0.03) %, Figure 1).

$$X = -4.59902 + 29.2024Y + 5.54816Y^2 \quad (1)$$

61B-Cy5.5 and hIgG-Cy5.5 were synthesized through the modification of amino groups. Based on the absorbance at 280 and 673 nm, the molar ratio of dye/61B and dye/hIgG was calculated to be 3.7 and 4.8, respectively.

Dll4 Binding with Tumor Cell Lines

Dll4 binding with U87MG and HT29 cell lines were analyzed by cell confocal microscopy image. As shown in Figure 2, intracellular fluorescence was observed in both U87MG and HT29 tumor cells incubated with 61B-Cy5.5; and U87MG cells showed higher fluorescence signal intensity as compared to HT29. However, no fluorescent signal was observed in IgG-Cy5.5 treated cells. In addition, binding of fluorescence labeled 61B can be successfully blocked by added access amount of nonlabeled 61B antibody (Supplementary Figure 6). Since 61B-Cy5.5 showed specific binding to both U87MG and HT29, both tumor xenografts were established and used for in vivo evaluation of 61B-DOTA-^{64}Cu.

MicroPET Imaging Study

The tumor targeting efficacy of 61B-DOTA-^{64}Cu was evaluated by multiple-time-point static MicroPET scans in U87MG and HT29 tumor-bearing mice. hIgG-DOTA-^{64}Cu was used as control (n = 4 per group). After intravenous injection of 61B-DOTA-^{64}Cu, both U87MG and HT29 tumor xenografts can be clearly visualized with good tumor-to-background contrast (Figure 3). The quantitative PET results were shown in Figure 4. For U87MG tumor, the uptake was 3.0 ± 0.6, 10.5 ± 1.7, and 10.2 ± 1.2%ID/g, at 1, 24, and 48 h after injection, respectively. For HT29 tumor, the uptake was 2.3 ± 0.3, 7.3 ± 1.3, and 6.6 ± 1.3%ID/g at 1, 24, and 48 h after injection, respectively. The U87MG tumor uptake of the probe was significantly higher than HT29 tumor at 24 and 48 h postinjection time points examined (p < 0.05, Figure 5A). Moreover, the tumor uptakes of hIgG-DOTA-^{64}Cu were significantly lower than that of 61B-DOTA-^{64}Cu at 24 and 48 h postinjection in both tumor models (p < 0.05, Figure 5B,C). At the first time points, both 61B-DOTA-^{64}Cu and hIgG-DOTA-^{64}Cu demonstrated high blood pool accumulation in two tumor models, which could be explained by the relative long circulation half-life of antibodies in vivo. At 24 h postinjection, the activity accumulation in blood pool decreased dramatically. The liver also showed relatively high uptake of both 61B-DOTA-^{64}Cu and hIgG-DOTA-^{64}Cu as a result of nonspecific uptake through the liver reticular-endothelial system. Muscle uptakes of both 61B-DOTA-^{64}Cu and hIgG-DOTA-^{64}Cu were minimal and not significantly different at all tested time points (Figure 4 and Supplementary Figure 4). In order to further validate the PET quantification, biodistribution by direct tissue sampling was obtained right after PET scans at 72 h postinjection (Supplementary Figure 3). The U87MG tumor uptake for 61B-DOTA-^{64}Cu and hIgG-DOTA-^{64}Cu was 8.1 ± 1.8 and 4.5 ± 1.4%ID/g, respectively. In contrast, uptake for other normal organs between 61B-DOTA-^{64}Cu and hIgG-DOTA-^{64}Cu showed similar results with no significant difference (p > 0.05) (Supplementary Table 1). The biodistribution results are consistent with PET quantification.

Immunofluorescence Staining of Tumor Tissues

To investigate the distribution of 61B or IgG within the tumor, tumor tissues were collected at 48 h after intravenous injection of 61B-Cy5.5 or IgG-Cy5.5. Frozen sections of tumors were stained for blood vessels with anti-CD31 antibody. As shown in Figure 6, the accumulation of 61B-Cy5.5 in the U87MG tumor tissues was significantly higher than that in HT29 tumor tissues. In addition, the distribution of 61B-Cy5.5 in HT29 tumor tissue was more proximate to CD31 positive tumor vessels. No significant distribution of hIgG-Cy5.5 was observed in either U87MG or HT29 tumor models. Both in vivo PET imaging data and in vitro data indicated that 61B could specifically and effectively bind to Dll4 expressed in the tumor models tested, especially in U87MG.

Discussion

Accumulating evidence indicates that Dll4 is a promising target for diagnosis, prognosis, and therapy in numerous cancer types.[8,16–18] Therefore, the ability to noninvasively visualize Dll4 expression in vivo could be of great clinical value in Dll4 based tumor management. For example, through noninvasive Dll4-targeted imaging, the expression of Dll4 can be assessed conveniently, and the changes of Dll4 expression during treatment

could be monitored. Obviously, these would aid in many procedures, including early lesion detection, prognostic evaluation, patient selection, better treatment monitoring, and dose optimization.[19]

Previously, the soluble forms of Dll4 or Dll4-Fc (sDll4 or sDll4-Fc) were used as the agent for Dll4-Notch pathway blocking.[3,20] However, both the tumor uptake and the pharmacokinetics of these probes need to be further improved. Furthermore, sDll4 or sDll4-Fc will inhibit the binding of all Notch and Notch ligands, including Dll1, Dll4, Jagged1, and Jagged2, which may introduce unwanted side effects. Monoclonal antibody is considered as potentially the most specific probe for imaging because it offers an unmatched ability to bind selectively to the target of interest.[21] Recently, anti-Dll4 antibodies have been used for Dll4-Notch pathway target management.[22–24] Due to the high binding activity and specificity, the antibody-based imaging probes would be more suitable for patient screening as they are closely related to the antibody drug to be used in therapy. In this study, we developed Dll4-targeted PET probes based on anti-Dll4 monoclonal antibodies. In our approach, a novel ^{64}Cu-labeled Dll4 antibody, 61B-DOTA-^{64}Cu, was synthesized and characterized. Binding activity assay showed that 61B-DOTA preserved (77.2 ± 3.7) % Dll4 binding activity as compared with unlabeled 61B. 61B-Cy5.5 was also synthesized, which can effectively bind to Dll4 positive U87MG and HT29 cells. Confocal laser scanning microscope imaging indicated that the antibody was mainly observed in the cytoplasm, which indicated that the antibody may get internalized upon binding to Dll4. Although the mechanism of internalization needs further investigation, it could be caused by Dll4-mediated endocytosis.[25] In contrast, hIgG-Cy5.5 showed almost no binding to both tumor cell lines. These evidence suggested that 61B could specifically bind to both U87MG and HT29 tumor cells.

We further tested Dll4 targeting efficacy of 61B-DOTA-^{64}Cu in U87MG and HT29 tumor bearing mice with microPET imaging. In both xenografts models, tumor uptake of 61B-DOTA-^{64}Cu increased with time, peaked at 24 h postinjection, and maintained at a relatively high level until 48 h postinjection. At 24 and 48 h postinjection, the tumor uptake was stable in U87MG model, but decreased slightly over time in HT29 tumor model. Furthermore, the probe uptake in U87MG tumor was significantly higher than that in HT29 tumor at 24 and 48 h postinjection. Both active uptake (as a result of Dll4-Notch interaction) and passive uptake (as a result of the enhanced permeability and retention effect) contributed to the probe accumulation in tumors. Because the IgG tumor uptake for U87MG and HT29 are comparable, the tumor uptake difference between U87MG and HT29 should be mainly caused by active targeting. As shown in Figure 2, U87MG tumor cell demonstrated stronger binding toward 61B-Cy5.5 compared with HT29 cell. Nonetheless, additional quantitative analysis needs to be performed to further confirm the cell surface Dll4 expression in these cell lines. Due to the limited availability of the antibody, blocking experiment with 61B was not performed in this study. In order to measure the specific targeting attributed to 61B antibody, hIgG-DOTA-^{64}Cu was used as the control. With a lack of active targeting capability, tumor accumulation of hIgG-DOTA-^{64}Cu represents passive uptake. As expected, the uptake of hIgG-DOTA-^{64}Cu at most time points examined was comparatively low in both tumor models, which confirms the target specificity of 61B-DOTA-^{64}Cu. To further validate the in vivo findings, we performed tumor tissue immunofluorescence staining of the

U87MG and HT29 tumor models at 48 h postinjection of 61B-Cy5.5 or hIgG-Cy5.5, respectively. The results clearly demonstrated that more 61B-Cy5.5 accumulated in U87MG tumor than in HT29 tumor. There was no significant distribution of hIgG-Cy5.5 in both tumor models. These results are consistent with in vivo microPET imaging studies. Interestingly, we also noticed that the 61B-Cy5.5 distribution in HT29 tumor tissue coincided with CD31 positive blood vessel distribution (Figure 6 and Supplementary Figure 5). According to the cell staining and in vivo imaging results, the 61B uptake in HT29 tumor cell was lower than that in U87MG tumor cell. 61B-Cy5.5 just distributed near the vessels in HT29 tumor model maybe because the antibody reaches this area. We do like to point out that 61B is the monoclonal antibody of human Dll4, which does not target murine Dll4 that may also be overexpressed on vasculature in xenograft mouse model. However, clinical application of Dll4/Notch pathway block treatment may not be limited to cancer cells that overexpress Dll4. Patients could benefit from this treatment if the tumor vasculature is Dll4 positive. Clearly, PET imaging could play an important role in the patient's selection. From another point of view, 61B-DOTA-^{64}Cu might show higher tumor uptake in future clinic applications because it recognizes both tumor cells and vasculature associated Dll4 expression. Accordingly, we believe that the antibody could be used in not only diagnosis but also theranostics by conjugated with radionuclides suitable for imaging and therapy (e.g., ^{90}Y, ^{177}Lu, or ^{161}Tb).[26]

Despite the success of this experimental in vitro and in vivo imaging study, there are still several open questions remaining to be addressed in the future work. First, the tumors also showed some uptake of hIgG-DOTA-^{64}Cu due to the presence of nonspecific accumulation. Therefore, the accumulation caused by “passive” targeting needs to be considered during data interpretation. Second, because of the relative large molecular size, the antibody usually takes longer time to optimally accrete in tumors.[27] Various antibody fragments with smaller molecular size have been developed, such as diabodies, minibodies, and some antibodies based on nontraditional scaffolds.[21,28,29] These ligands might offer other alternatives for Dll4 targeted tumor imaging in future clinical application. And last, although we have demonstrated that the expression level of Dll4 was higher in U87MG cells than in HT29 cells, we failed to detect the desired 75–80 kDa band corresponding to human Dll4 using commercial available rabbit antihuman Dll4 antibody by Western blot. We also tried to using 61B to probe Dll4 in cell lysate. However, the nonspecific binding was dominant due to the fact that 61B is a humanized antibody and HRP labeled antihuman secondary antibody needs to be used for membrane development. Clearly, Western blot analysis of Dll4 in human glioma U87MG and colorectal cancer HT29 cell lines will need to be further optimized using other antibodies. We will try antibodies from other vendors in our follow-up studies.

Conclusion

We have described the in vitro and in vivo distribution of ^{64}Cu labeled Dll4 antibody in glioblastoma and colorectal cancer models. This approach would be valuable for tumor detecting, evaluating the Dll4 expression, and monitoring the Dll4-based cancer therapies. Moreover, the newly developed probe might also have potential applications in other cancer types expressing Dll4.

Supplementary Material

Refer to Web version on PubMed Central for supplementary material.

Acknowledgments

This work was supported by the 1R01EB014354-01A1 (NIBIB), P30-CA016086-35-37 (NCI), the American Cancer Society (12199ss1-MRSG-12-034-01-CCE), National Natural Science Foundation of China (No. U1032002, 81271621, 81301266, 81430041), and Key Clinical Research Project of Public Health Ministry of China 2010-2012 (No. 164).

References

1. Takeuchi H, Haltiwanger RS. Role of glycosylation of Notch in development. Semin Cell Dev Biol. 2010; 21(6):638–45. [PubMed: 20226260]
2. Li JL, Sainson RC, Shi W, Leek R, Harrington LS, Preusser M, Biswas S, Turley H, Heikamp E, Hainfellner JA, Harris AL. Delta-like 4 Notch ligand regulates tumor angiogenesis, improves tumor vascular function, and promotes tumor growth in vivo. Cancer Res. 2007; 67(23):11244–53. [PubMed: 18056450]
3. Scehnet JS, Jiang W, Kumar SR, Krasnoperov V, Trindade A, Benedito R, Djokovic D, Borges C, Ley EJ, Duarte A, Gill PS. Inhibition of Dll4-mediated signaling induces proliferation of immature vessels and results in poor tissue perfusion. Blood. 2007; 109(11):4753–60. [PubMed: 17311993]
4. Miyamoto S, Rosenberg DW. Role of Notch signaling in colon homeostasis and carcinogenesis. Cancer Sci. 2011; 102(11):1938–42. [PubMed: 21801279]
5. Gale NW, Dominguez MG, Noguera I, Pan L, Hughes V, Valenzuela DM, Murphy AJ, Adams NC, Lin HC, Holash J, Thurston G, Yancopoulos GD. Haploinsufficiency of delta-like 4 ligand results in embryonic lethality due to major defects in arterial and vascular development. Proc Natl Acad Sci U S A. 2004; 101(45):15949–54. [PubMed: 15520367]
6. Zhang JX, Cai MB, Wang XP, Duan LP, Shao Q, Tong ZT, Liao DZ, Li YY, Huang MY, Zeng YX, Shao JY. Elevated DLL4 expression is correlated with VEGF and predicts poor prognosis of nasopharyngeal carcinoma. Med Oncol. 2013; 30(1):390. [PubMed: 23275120]
7. Liu SK, Bham SA, Fokas E, Beech J, Im J, Cho S, Harris AL, Muschel RJ. Delta-like ligand 4-notch blockade and tumor radiation response. J Natl Cancer Inst. 2011; 103(23):1778–98. [PubMed: 22010178]
8. Hu W, Lu C, Dong HH, Huang J, Shen DY, Stone RL, Nick AM, Shahzad MM, Mora E, Jennings NB, Lee SJ, Roh JW, Matsuo K, Nishimura M, Goodman BW, Jaffe RB, Langley RR, Deavers MT, Lopez-Berestein G, Coleman RL, Sood AK. Biological roles of the Delta family Notch ligand Dll4 in tumor and endothelial cells in ovarian cancer. Cancer Res. 2011; 71(18):6030–9. [PubMed: 21795478]
9. Zoller F, Markert A, Altmann A, Mier W, Haberkorn U. Identification of a novel anti-DLL4 cystine-knot miniprotein for tumor imaging using ribosome display technology. J Nucl Med. 2012; 53(supplement 1):24.
10. Li ZB, Cai W, Cao Q, Chen K, Wu Z, He L, Chen X. (64)Cu-labeled tetrameric and octameric RGD peptides for small-animal PET of tumor alpha(v)beta(3) integrin expression. J Nucl Med. 2007; 48(7):1162–71. [PubMed: 17574975]
11. Liu S, Li D, Park R, Liu R, Xia Z, Guo J, Krasnoperov V, Gill PS, Li Z, Shan H, Conti PS. PET imaging of colorectal and breast cancer by targeting EphB4 receptor with 64Cu-labeled hAb47 and hAb131 antibodies. J Nucl Med. 2013; 54(7):1094–100. [PubMed: 23667241]
12. Li D, Liu S, Liu R, Zhou Y, Park R, Naga K, Krasnoperov V, Gill PS, Li Z, Shan H, Conti PS. EphB4-targeted imaging with antibody h131, h131-F(ab′)2 and h131-Fab. Mol Pharmaceutics. 2013; 10(12):4527–33.
13. Li D, Liu S, Liu R, Park R, Hughes L, Krasnoperov V, Gill PS, Li Z, Shan H, Conti PS. Targeting the EphB4 receptor for cancer diagnosis and therapy monitoring. Mol Pharmaceutics. 2013; 10(1): 329–36.

14. Liu S, Li D, Guo J, Canale N, Li X, Liu R, Krasnoperov V, Gill PS, Conti PS, Shan H, Li Z. Design, synthesis, and validation of Axl-targeted monoclonal antibody probe for microPET imaging in human lung cancer xenograft. Mol Pharmaceutics. 2014; 11(11):3974–9.
15. Wu Y, Zhang X, Xiong Z, Cheng Z, Fisher DR, Liu S, Gambhir SS, Chen X. microPET imaging of glioma integrin {alpha}v{beta}3 expression using (64)Cu-labeled tetrameric RGD peptide. J Nucl Med. 2005; 46(10):1707–18. [PubMed: 16204722]
16. Li ZQ, Gong LL, Wen ZH, Wang J, Xu CS, Huang XD. Delta-like ligand 4 correlates with endothelial proliferation and vessel maturation in human malignant glioma. Onkologie. 2012; 35(12):763–8. [PubMed: 23207622]
17. Koukourakis MI, Giatromanolaki A, Sivridis E, Gatter KC, Harris AL. High DLL4 expression in tumour-associated vessels predicts for favorable radiotherapy outcome in locally advanced squamous cell head-neck cancer (HNSCC). Angiogenesis. 2013; 16(2):343–51. [PubMed: 23108591]
18. Kontomanolis E, Panteliadou M, Giatromanolaki A, Pouliliou S, Efremidou E, Limberis V, Galazios G, Sivridis E, Koukourakis MI. Delta-like ligand 4 (DLL4) in the plasma and neoplastic tissues from breast cancer patients: correlation with metastasis. Med Oncol. 2014; 31(5):945. [PubMed: 24696220]
19. Cai W, Rao J, Gambhir SS, Chen X. How molecular imaging is speeding up antiangiogenic drug development. Mol Cancer Ther. 2006; 5(11):2624–33. [PubMed: 17121909]
20. Djokovic D, Trindade A, Gigante J, Badenes M, Silva L, Liu R, Li X, Gong M, Krasnoperov V, Gill PS, Duarte A. Combination of Dll4/Notch and Ephrin-B2/EphB4 targeted therapy is highly effective in disrupting tumor angiogenesis. BMC Cancer. 2010; 10:641. [PubMed: 21092311]
21. Kaur S, Venktaraman G, Jain M, Senapati S, Garg PK, Batra SK. Recent trends in antibody-based oncologic imaging. Cancer Lett. 2012; 315(2):97–111. [PubMed: 22104729]
22. Yen WC, Fischer MM, Hynes M, Wu J, Kim E, Beviglia L, Yeung VP, Song X, Kapoun AM, Lewicki J, Gurney A, Simeone DM, Hoey T. Anti-DLL4 has broad spectrum activity in pancreatic cancer dependent on targeting DLL4-Notch signaling in both tumor and vasculature cells. Clin Cancer Res. 2012; 18(19):5374–86. [PubMed: 22952347]
23. Koga J, Aikawa M. Application of anti-ligand antibodies to inhibit Notch signaling. Methods Mol Biol. 2014; 1187:335–42. [PubMed: 25053501]
24. Jenkins DW, Ross S, Veldman-Jones M, Foltz IN, Clavette BC, Manchulenko K, Eberlein C, Kendrew J, Petteruti P, Cho S, Damschroder M, Peng L, Baker D, Smith NR, Weir HM, Blakey DC, Bedian V, Barry ST. MEDI0639: a novel therapeutic antibody targeting Dll4 modulates endothelial cell function and angiogenesis in vivo. Mol Cancer Ther. 2012; 11(8):1650–60. [PubMed: 22679110]
25. De Biasio A, Guarnaccia C, Popovic M, Uversky VN, Pintar A, Pongor S. Prevalence of intrinsic disorder in the intracellular region of human single-pass type I proteins: the case of the notch ligand Delta-4. J Proteome Res. 2008; 7(6):2496–506. [PubMed: 18435556]
26. Cutler CS, Hennkens HM, Sisay N, Huclier-Markai S, Jurisson SS. Radiometals for combined imaging and therapy. Chem Rev. 2013; 113(2):858–83. [PubMed: 23198879]
27. Kelloff GJ, Krohn KA, Larson SM, Weissleder R, Mankoff DA, Hoffman JM, Link JM, Guyton KZ, Eckelman WC, Scher HI, O'Shaughnessy J, Cheson BD, Sigman CC, Tatum JL, Mills GQ, Sullivan DC, Woodcock J. The progress and promise of molecular imaging probes in oncologic drug development. Clin Cancer Res. 2005; 11(22):7967–85. [PubMed: 16299226]
28. Sheridan C. Pharma consolidates its grip on post-antibody landscape. Nat Biotechnol. 2007; 25(4): 365–6. [PubMed: 17420728]
29. Holliger P, Hudson PJ. Engineered antibody fragments and the rise of single domains. Nat Biotechnol. 2005; 23(9):1126–36. [PubMed: 16151406]

Abbreviations

Dll4	delta-like ligand 4
PET	positron emission tomography

Dll4-AP	Dll4-alkaline phosphatase
DOTA	1,4,7,10-tetra-azacyclododecane-*N*,*N*′,*N*″,*N*‴-tetraacetic acid
hIgG	human IgG
DMEM	Dulbecco's minimum essential medium
PBS	phosphate buffered saline
NHS	*N*-hydroxysuccinimide
FBS	fetal bovine serum
DAPI	4,6-diamino-2-phenylindole
sDll4	soluble forms of Dll4
%ID/g	percentage injected dose per gram

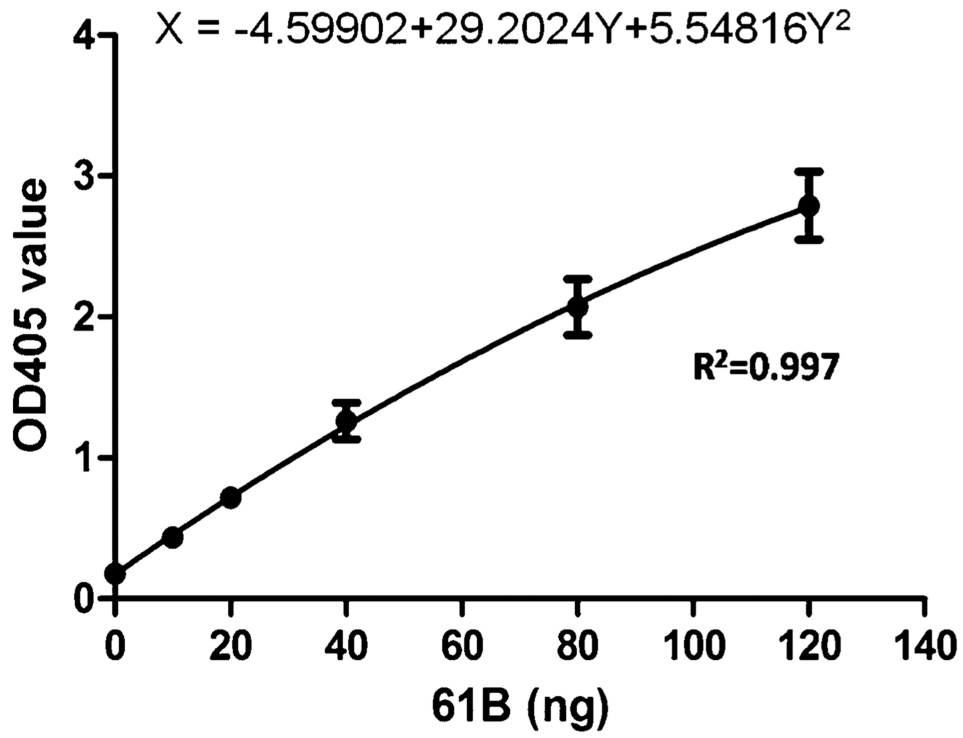

Figure 1.
Standard curve and mathematical formula of binding activity.

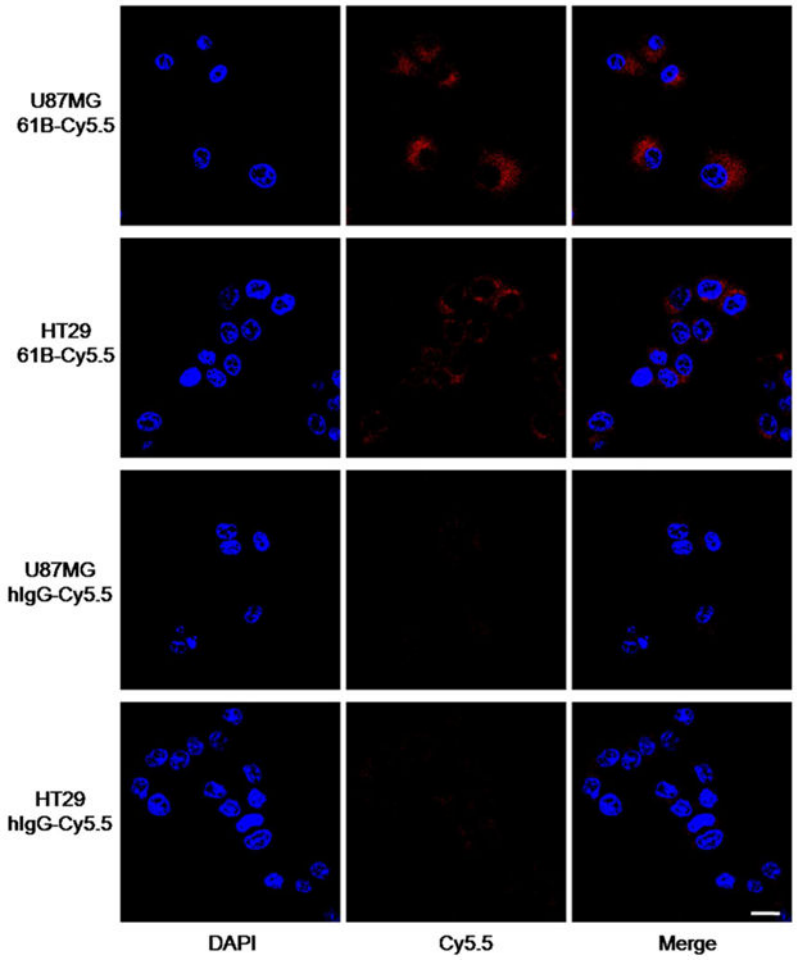

Figure 2.

Confocal analysis of the antibody distribution in U87MG and HT29 cells. The cells were incubated with 61B-Cy5.5 or hIgG-Cy5.5 at 37 °C for 30 min. Images were obtained under identical conditions and displayed at the same magnification (×630). Scale bar = 20 μm.

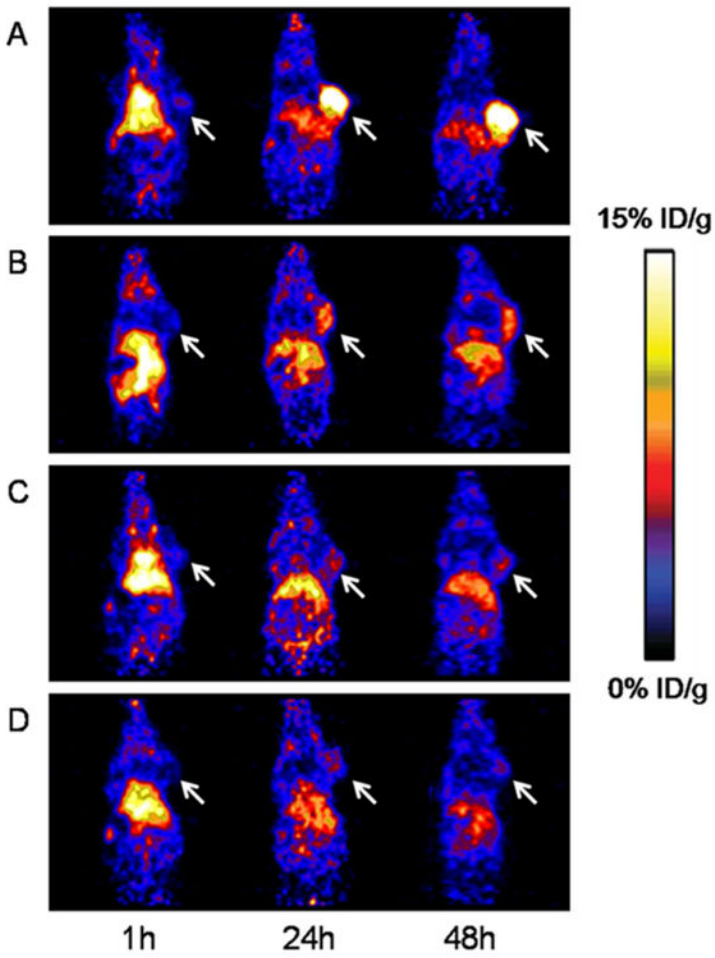

Figure 3.

Decay-corrected whole-body coronal small-animal PET images from static scans at 1, 24, and 48 h postinjection of (A) 61B-DOTA-^{64}Cu into U87MG tumor model, (B) 61B-DOTA-^{64}Cu into HT29 tumor model, (C) hIgG-DOTA-^{64}Cu into U87MG tumor model, and (D) hIgG-DOTA-^{64}Cu into HT29 tumor model. Tumors are indicated by white arrows.

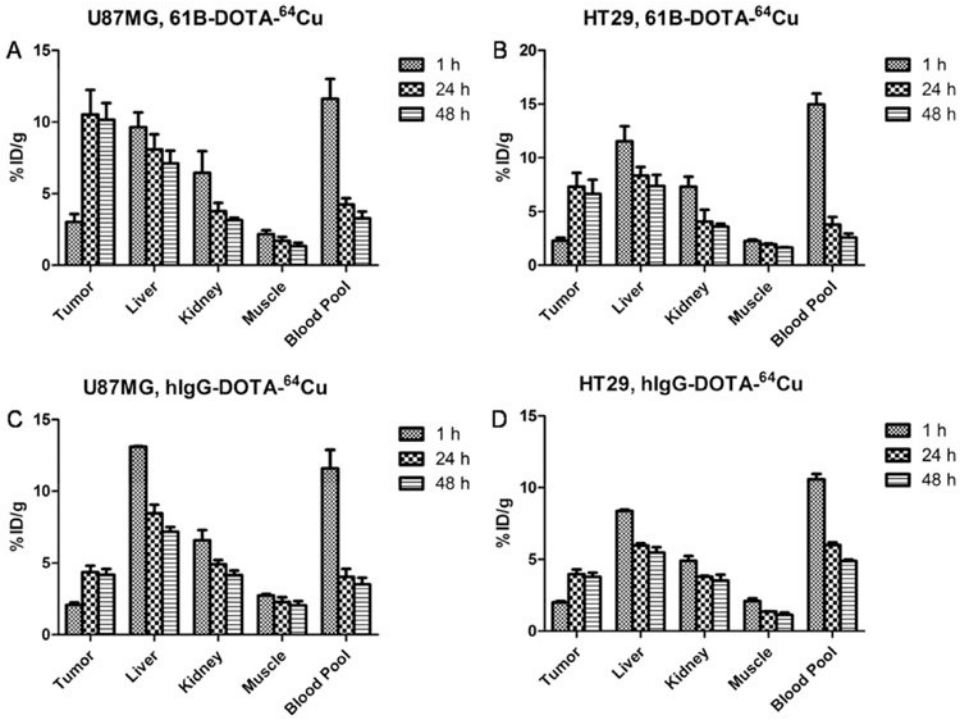

Figure 4.

Tumor and major organ radioactivity accumulation quantification from a static scan at 1, 24, and 48 h postinjection of (A) 61B-DOTA-^{64}Cu into U87MG tumor model, (B) 61B-DOTA-^{64}Cu into HT29 tumor model, (C) hIgG-DOTA-^{64}Cu into U87MG tumor model, and (D) hIgG-DOTA-^{64}Cu into HT29 tumor model. Data are expressed as average ± SD.

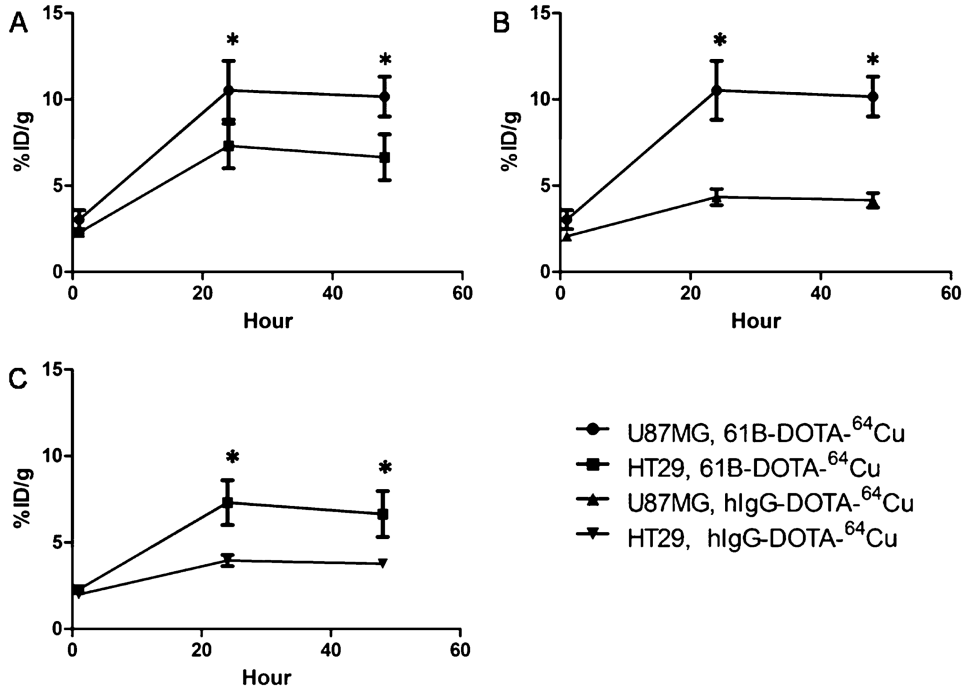

Figure 5.

Time course of tumor uptake from 1 to 48 h postinjection. (A) U87MG and HT29 tumor uptake of 61B-DOTA-^{64}Cu. (B) U87MG tumor uptake of 61B-DOTA-^{64}Cu and hIgG-DOTA-^{64}Cu. (C) HT29 tumor uptake of 61B-DOTA-^{64}Cu and hIgG-DOTA-^{64}Cu. Data are expressed as average ± SD, and the p value was calculated with Student's t test (*$p < 0.05$).

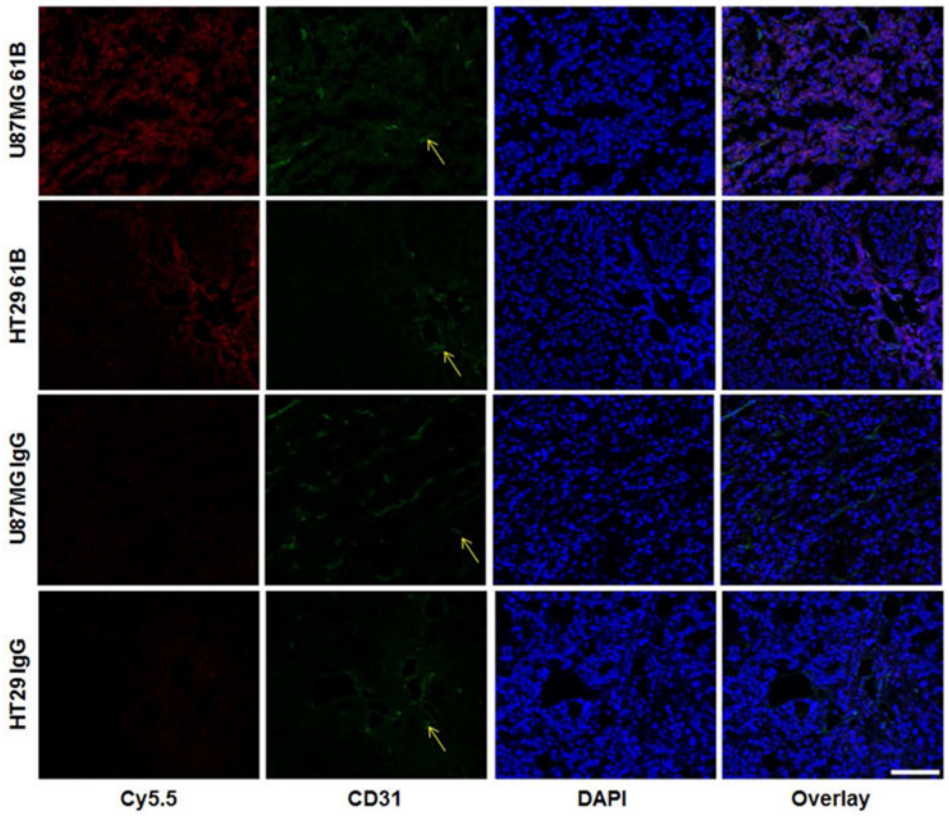

Figure 6.

Confocal fluorescence of 61B-Cy5.5 and immunofluorescence staining of CD31 in U87MG and HT29 tumor tissues. Arrows indicated the blood vessels. Images were obtained under identical conditions and displayed at the same magnification (×200). Scale bar = 100 μm.